공학석사 학위논문

유한요소 모델링 기반 소프트로봇 실시간 상태 및 외력추정

A Real-time State and Disturbance Estimation Approach for Soft Robots with Finite Element Method Modelling

2021년 2월

서울대학교 대학원

기계항공공학부

홍 일 권

유한요소 모델링 기반 소프트로봇 실시간 상태 및 외력추정

A Real-time State and Disturbance Estimation Approach for Soft Robots with Finite Element Method Modelling

지도교수 이 동 준

이 논문을 공학석사 학위논문으로 제출함
2021년 2월

서울대학교 대학원
기계항공공학부
홍 일 권

홍일권의 석사 학위논문을 인준함
2021년 2월

위 원 장 이 경 수 (인)

부위원장 이 동 준 (인)

위 원 조 규 진 (인)

Abstract

A Real-time State and Disturbance Estimation Approach for Soft Robots with Finite Element Method Modelling

Ilkwon Hong
Mechanical & Aerospace Engineering
The Graduate School
Seoul National University

Perception of soft robot is essential to enhance the performance and the ability of soft robots in real world application such as manipulation, and locomotion. We propose a real-time state and disturbance estimation algorithm for soft robots. First, we model soft robot dynamics using linear finite element method(FEM) and perform balanced model reduction(BMR) for given contact and actuation mode. Then, for the case where there exist no internal actuation, we propose a state and disturbance estimation algorithm based on least square with additional energy cost and state projection. Finally, when internal actuation exists, with the assumption of random walk disturbance we formulate a filtering based estimation that simultaneously estimates state and disturbance. The performance of the algorithm is tested by simulations and experiments.

Keywords: Balanced model reduction, Finite element method, Optimization, Filtering, Soft robotics
Student Number:2018-21160

Acknowledgements

연구실에 입학한지 벌써 2년 반이 지나 졸업을 앞두고 있게 되었습니다. 여전히 스스로의 모습이 만족스럽진 않지만 석사과정을 거치며 많은 발전을 이루었고 앞으로의 방향성에 대해 실마리를 잡은 것 같다 생각합니다.

연구실에서 생활하며 많은 사람들의 도움을 받을 수 있었습니다. 먼저 석사과정 동안 많은 가르침을 주신 이동준 교수님께 감사의 말씀을 드립니다. 연구에 관한 것 뿐만 아니라 평상시의 태도에서부터 성실하고 꼼꼼함을 추구하는 교수님의 철학과 충고는 항상 저를 돌아보며, 앞으로의 사회생활과 연구에 있어 저의 큰 자산이 될 것이라고 생각합니다.

연구실에서의 생활을 통해 값진 동료들을 만날 수 있었습니다. 함께 연구실 생황을 하면서 많은 자극을 받을 수 있었고, 연구 뿐만 아니라 인생과 관련한 많은 이야기를 나눌 수 있었던 시간이었던 것 같습니다.

대학원 생활을 하면서 항상 저에게 힘이 되며 조언을 해 주고 정신적으로 성숙해지는데 큰 도움이 된 예슬이에게 고마움의 말을 전합니다.

마지막으로 저를 믿고 지원해주신 부모님에게 감사의 말씀 전합니다. 굳건한 마음으로 정진하여 발전하는 모습을 보여드리도록 하겠습니다. 감사합니다.

2021년 2월

홍일권

Contents

List of Figures

Abbreviations

BMR	**B**alanced **M**odel **R**eduction
FEM	**F**inite **E**lement **M**ethod
PMI	**P**assive **M**idpoint **I**ntegration

Chapter 1

Introduction

Soft robotics is rapidly growing field. Due to its elastic nature, these robots can be used in applications such as human safe interaction, and locomotion in tough, unstructured environment[1],[2],[3]. However, its application to tasks such as precise control and the performance shown is still in early stages.

In order to enhance the performance of soft robot, the perception issue is a challenge to be solved. Perception is an ability to reconstruct current shape and configuration. There are two kinds of perception: proprioception, the ability to perceive its own state and exteroception, the ability to feel external stimuli[4]. Perception is an essential component for an autonomous system because it is necessary to use feedback and closed-loop control techniques.

The main challenges in soft robot perception are due to its high dimensionality. Commonly used methods for proprioception can be divide into the following three: 1) learning based method using camera or strain sensors [5],[6], [7] 2) using a simplified model such as piece wise constant curvature(PCC) model[8],[9],[10], or cosserat theory[11] and 3) using FEM model[12]. Using camera incorporating with machine learning technique can handle large information without formulating model dynamics. However, this technique has no intuition about the motion, and there is no guarantee that the estimation is always precise. Additionally, adopting camera sensor can be limited for application in tough condition because of occlusion or light change. Simplifying the robot modelling by adopting assumptions like PCC, fits well in some cases like invasive surgery robot. However, this can be applied only to very specific shaped model, and as the model gets complicated the accuracy will be degraded. Using FEM to model the soft robot is much more general and accurate method. The main downside of this method is it cannot be applied to real-time application because of the large dimension of FEM dynamics.

For exteroception of soft robot, internal camera with learning technique[13], and soft tactile sensor array[14] is commonly used. Additional space for tactile sensing is needed for internal camera method. For tactile sensor array, the whole body should be covered with sensors and there can be fabrication issues such as wiring or cost problem. Also, there are some observer based method[9],[12]. However, [12] adopted external sensor such as vision sensing. For the case of [9] simplified PCC model is adopted and the algorithm is limited to static case.

In this thesis we adopt FEM with BMR to model soft robot with high accuracy while enabling real-time estimation. Then, we embedded some low-cost on-board sensors such as IMU on soft robot, which is free with occlusion and fabrication issue. With the proposed algorithm, we could perform real-time state and disturbance estimation such as contact force without the need of additional tactile sensors.

The rest of the thesis is organized as follows. Chapter 2 contains some preliminary materials, including the concept of FEM, and BMR. Chapter 3 contains the summary of estimation algorithms. Chapter 4 shows the simulation results. Experiment results are in Chapter 5 and Chapter 6 include concluding remarks.

The contributions of this study are as following 1)real-time state and disturbance estimation algorithm based on FEM dynamics is developed, 2) estimation is performed with onboard sensors.

Chapter 2

System Modeling for Soft Object

2.1 FEM Modelling

We adopted FEM to model the soft robot, which is demonstrated by finite number of nodes[15]. The position of l-th node is defined by $p_l := [p_l^x, p_l^y, p_l^z] \in \mathbb{R}^3$ Then the entire configuration of the soft robot can be represented by

$$x := [p_1; p_2; \cdots; p_N] \in \mathbb{R}^n \tag{2.1}$$

Where N represents the total number of FEM nodes, and $n = 3N$ is the total dimension of the dynamics.

Adopting this as state, the total dynamics of the soft robot can be written as

$$M\ddot{x} + C\dot{x} + Kx = P_a + A_e f_e \tag{2.2}$$

$M, C, K \in \mathbb{R}^{n \times n}$ are the inertia, damping and stiffness matrices of the soft robot, all symmetric and positive definite. P_a represents the actuation vector of soft robot. $f_e \in \mathbb{R}^q$ represents the contact forcing term and $A_e \in \mathbb{R}^{n \times q}$ is the disturbance matrix specifying the subset of nodes where the disturbance f_e is applied. We omitted the gravity term for simplicity.

In this thesis we adopted linear FEM model. Therefore, we assumed that M, C, K is constant matrix. This assumption fits well in small deformation. In case of large deformation we can adopt additional technique such as model switching algorithm[16] and, this will be dealt as future work.

2.2 Balanced Model Reduction

The dimension of the full-order FEM model equation (2.2) is large to handle in real-time application. Therefore, model reduction technique is needed to reduce the calculation burden. In soft robotics the data driven method such as PCA/-POD is frequently used to perform model reduction[17],[18],[19]. However, in this

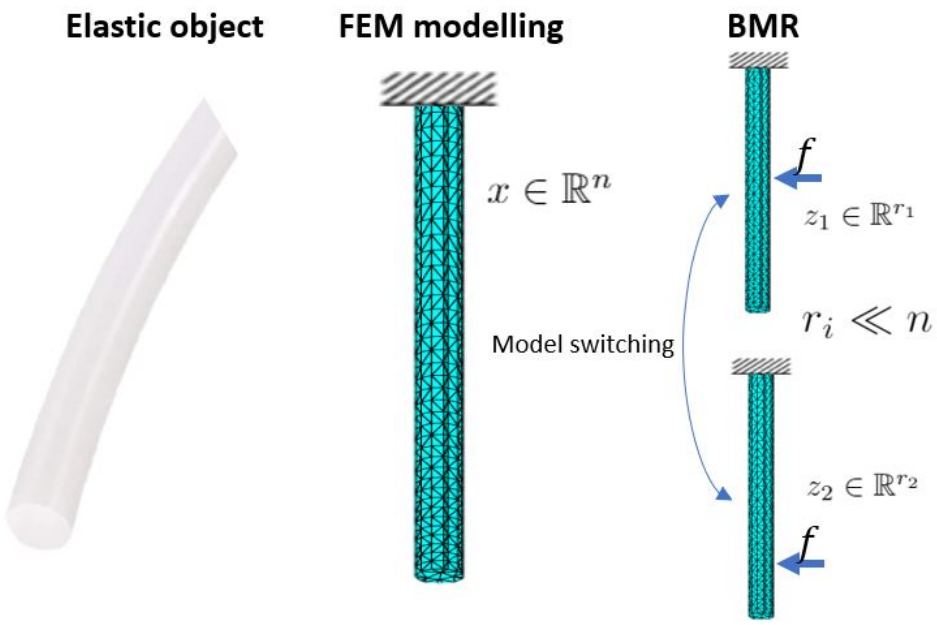

FIGURE 2.1: The idea of balanced model reduction and switching

thesis we chose BMR method[20],[21] to perform model reduction since it is an analytical technique, therefore more efficient to handle complicated cases (e.g. soft robot that has multiple actuation with several contacts).

As shown in figure 2.1 our model reduction idea is to perform a BMR for each different contact case. Then, we can use each reduced model that correspond to current contact case. When the contact changes, we can incorporate model switching algorithm to handle the change of motion. This method is much more efficient than representing the whole available motion with one model.

In order to perform BMR, we first reformulate the full order FEM dynamics (2.2), into first-order state-space form

$$\begin{bmatrix} M & 0 \\ 0 & I \end{bmatrix} \begin{bmatrix} \ddot{x} \\ \dot{x} \end{bmatrix} = \begin{bmatrix} -C & -K \\ I & 0 \end{bmatrix} \begin{bmatrix} \dot{x} \\ x \end{bmatrix} + \begin{bmatrix} P_a + A_e f_e \\ 0 \end{bmatrix} \tag{2.3}$$

The main goal of this thesis is estimation of the shape and disturbance, so we chose x as an output and $P_a + A_e f_e$ as an output. Then we can compute the controllability and observability gramian.

$$W_C = \begin{bmatrix} W_{C,vv} & W_{C,vx} \\ W_{C,xv} & W_{C,xx} \end{bmatrix}, W_O = \begin{bmatrix} W_{O,vv} & W_{O,vx} \\ W_{O,xv} & W_{O,xx} \end{bmatrix} \tag{2.4}$$

All block matrices are $(n \times n)$-dimensional matrices. We then choose only $W_{C,xx}$,$W_{O,xx}$ which are relevant to the soft robot state. Then we can perform balanced realization as if this is the only state of the system

$$x := U\xi, U := R^T V \Lambda^{-\frac{1}{2}} \in \mathbb{R}^{n \times n} \tag{2.5}$$

Where $R^T R := W_{C,xx}, U\Lambda^2 U^T := R^T W_{O,xx} R$, and $U^T = U^T U = I$. Matrix Λ contains Hankel singular values of controllability and observability Gramians of transformed state $\xi \in \mathbb{R}^n$,where $W_{C,\xi\xi} = W_{O,\xi\xi} = \Lambda$.

Then we reduce the dimension using dominant component of ξ, by selecting first r largest Hankel values as following

$$\xi_1 := P_1\xi \in \mathbb{R}^r, \xi_2 := P_2\xi \in \mathbb{R}^{n-r} \tag{2.6}$$

Where $P_1 = [I_{r\times r}, 0_{r\times n-r}] \in \mathbb{R}^{r\times n}$ is selection matrix for dominant component of state, and $P_2 = [0_{n-r\times r}, I_{n-r\times n-r}] \in \mathbb{R}^{n-r\times n}$ is for non-dominant state. The dimension r is chosen to be large enough to retain the accuracy of the model reduction, while also being small enough for real time estimation

Chapter 3

State and Disturbance Estimation Algorithms

3.1 Optimization Based Estimation

3.1.1 State Estimation

The node position x, which represents shape of the soft object can be represented by (2.5) and through (2.6) we can denote x as [16],[22]

$$x := U\xi \approx UP_1\xi_1 := U_1\xi_1 \tag{3.1}$$

To perform state and disturbance estimation using onboard sensors, we adopted IMU sensors to obsZerve current state of soft object. Taking y as an observation from IMU sensors, we can represent y as

$$y = Hx + v \approx HU_1\xi_1 + v' \tag{3.2}$$

Where $H \in \mathbb{R}^{6m\times n}$ is observation matrix, m represents the number of IMUs, and $v(0, V)$ is the Gaussian sensing noise. Detailed information about H is represented in Chapter 4. Here, we considered non-dominant components as additional noise $v'(0, C_y)$, which can be easily calculated as $C_y = V + (HU_2)^T \mathbb{E}\left(\Sigma\xi_2\xi_2^T\right) HU_2 \in \mathbb{R}^{3m\times 3m}$. In least square sense, we define a new cost function that contains measurement error term and potential energy term as following

$$F(\xi_1) = (HU_1\xi_1 - y)^T (HU_1\xi_1 - y) + \lambda_e (U_1\xi_1)^T KU_1\xi_1 \tag{3.3}$$

Where λ_e is energy cost gain. Then, by finding ξ_1 that minimizes the cost function (3.3), we can find optimal state estimation in least square sense. Then, full order state can be reconstructed from the minimization result of (3.3) and (2.5) as following.

$$\hat{\xi}_1 = \min_{\xi_1}(F) = \left(U_1^T H^T HU_1 + \lambda_E U_1^T KU_1\right)^{\ddagger} U_1^T H^T y \tag{3.4}$$

3.1.2 Disturbance Estimation

Based on the optimized state estimation $\hat{\xi}_1$ from (3.4) full order state x can be reconstructed as $\hat{x} = U_1\hat{\xi}_1$. Then, we incorporate quasi-static assumption and disturbance space projection to perform disturbance estimation.

From the quasi-static assumption, the state can be calculated by $x = K^{-1}A_e f_e$ (no actuation for soft object). However, reconstructed shape is not smooth because the cost function contains sensor noise. Direct substitution of this estimation into quasi static equation may result in force overfitting. Therefore, we project estimated state $\hat{x}$ onto the disturbance space (column space of $K^{-1}A_e$) which is available space in given input matrix, and calculate the interaction force through the projected state estimation.

$$\begin{aligned}
\tilde{x} &= K^{-1}A_e\left[\left(K^{-1}A_e\right)^T\left(K^{-1}A_e\right)\right]^{-1}\left(K^{-1}A_e\right)^T\hat{x} \\
\hat{f}_e &= K\tilde{x} \\
&= A_e\left[\left(K^{-1}A_e\right)^T\left(K^{-1}A_e\right)\right]^{-1}\left(K^{-1}A_e\right)^T U_1\hat{\xi}_1
\end{aligned} \tag{3.5}$$

The matrix on the right hand side can be calculated offline. Therefore, real-time state and disturbance estimation is available.

3.2 Filtering Based Estimation

3.2.1 Filtering Formulation with Augmented State

For optimization based estimation, we estimated state by error with energy minimization and disturbance by quasi-static assumption. For soft robot state and disturbance estimation, this cannot be easily implemented because of internal actuation. Therefore, we adopted Kalman filtering formulation with the random walk disturbance assumption. For this formulation, we first obtain the reduced dynamics based on the model reduction result via BMR (2.5),(2.6).

$$\bar{M}\ddot{\xi}_1 + \bar{C}\dot{\xi}_1 + \bar{K}\xi_1 = U_1^T P_a + U_1^T A_e f_e \tag{3.6}$$

where

$$\bar{M} = U_1^T M U_1,\ \bar{C} = U_1^T C U_1,\ \bar{K} = U_1^T K U_1, \tag{3.7}$$

Then using the PMI integration[23],[24] the reduced dynamics (3.6) can be discretized while enforcing discrete-time passivity.

$$\overbrace{(\frac{\bar{M}}{T} + \frac{\bar{C}}{2} + \frac{\bar{K}T}{4})}^{M_1}\dot{\xi}_{1,k+1} + \overbrace{(-\frac{\bar{M}}{T} + \frac{\bar{C}}{2} + \frac{\bar{K}T}{4})}^{M_2}\dot{\xi}_{1,k} + \bar{K}\xi_{1,k} = U_1^T P_{a,k} + U_1^T A_e f_{e,k} \tag{3.8}$$

Lowerscript k represents $k-th$ step value. Using this discretized dynamics, we can formulate the standard first-order state-space form as following

$$
\begin{aligned}
Z_{k+1} = \begin{bmatrix} \dot{\xi}_{1,k+1} \\ \xi_{1,k+1} \end{bmatrix} &= \overbrace{\begin{bmatrix} -M_1^{-1}M_2 & -M_1^{-1}\bar{K} \\ \frac{T}{2}\left(I - M_1^{-1}M_2\right) & I - \frac{T}{2}M_1^{-1}\bar{K} \end{bmatrix}}^{A_1} \begin{bmatrix} \dot{\xi}_{1,k} \\ \xi_{1,k} \end{bmatrix} \\
&+ \overbrace{\begin{bmatrix} M_1^{-1}U_1^T \\ M_1^{-1}U_1^T\frac{T}{2} \end{bmatrix}}^{A_2} A_e f_{e,k} + \overbrace{\begin{bmatrix} M_1^{-1}U_1^T \\ M_1^{-1}U_1^T\frac{T}{2} \end{bmatrix}}^{A_3} A_e P_{a,k}
\end{aligned}
\tag{3.9}
$$

Now we define an augmented state that contains state $\dot{\xi}_{1,k}$, $\xi_{1,k}$, and disturbance $f_{e,k}$ s.t.

$$
X_k = \begin{bmatrix} \dot{\xi}_{1,k} \\ \xi_{1,k} \\ f_{e,k} \end{bmatrix} = \begin{bmatrix} Z_k \\ f_{e,k} \end{bmatrix} \tag{3.10}
$$

Finally, incorporating random walk disturbance assumption, we can formulate dynamic propagation equation using augmented state as following

$$
X_{k+1} = \begin{bmatrix} A_1 & A_2 \\ 0 & I \end{bmatrix} X_k + \begin{bmatrix} A_3 \\ 0 \end{bmatrix} P_{a,k} + \begin{bmatrix} 0 \\ n_f \end{bmatrix} \tag{3.11}
$$

$n_f \sim N\left(0, C_f\right)$, where $C_f$is the covariance of the disturbance.

For state measurements we incorporate IMU sensors to update the propagation.

Like (3.2), we can formulate the update equation

$$y_k = \begin{bmatrix} HU_1 & 0 & 0 \\ 0 & HU_1 & 0 \end{bmatrix} X_k + e \tag{3.12}$$

Where e denotes the measurement noise.

3.2.2 Observability Analysis

For sensor placement, we first found out the minimum number of sensors required to satisfy HU_1 is a full rank matrix. From equation (3.11) and (3.12), the observability matrix can be calculated as following

$$\begin{bmatrix} HU_1 & 0 & 0 \\ 0 & HU_1 & 0 \\ & & C'A_2 \\ \vdots & \vdots & C'A_1A_2 + C'A_2 \\ & & \vdots \end{bmatrix} = \begin{bmatrix} O & O' \end{bmatrix} \tag{3.13}$$

Where $C' = \begin{bmatrix} HU_1 & 0 \; ; \; 0 & HU_1 \end{bmatrix}$. We choose the number of IMU to guarantee $O = \begin{bmatrix} HU_1 & 0 \; ; \; 0 & HU_1; \cdots \end{bmatrix}$, which is left two column of matrix, is a full rank matrix. Assume that there exists a nullspace of O', then we can find a vector $v \; s.t \; v \in N\left(C'A_2\right)$. Matrix C' is a full rank matrix, $v \in N\left(C'A_2\right) = N\left(A_2\right)$. Therefore, this unobservable vector v represents the force applied through the nullspace of A_2. However, this force will not affect the reduced dynamics, so

we can ignore these components. Ignoring these components, the system is observable, and we can simultaneously estimate the state and disturbance through Kalman filter formulation using (3.11) and (3.12).

Chapter 4

Simulation Results

4.1 General Elastic Object Simulation

Before examining our algorithms with real-world experiment, we performed simulations to verify the algorithm performance. As the purpose of our study is to estimate the shape and disturbance of soft object, we first performed simulation about general shape elastic object. We adopted simple cylinder shaped silicone rubber for the general shape case. The length of this silicone cylinder is $0.15m$ and the diameter of the cross section is $0.01m$, and we assumed that the material is isotropic. We first chose the Young's modulus, density, and the poison's ratio according to well known material property of silicone. This value is corrected for

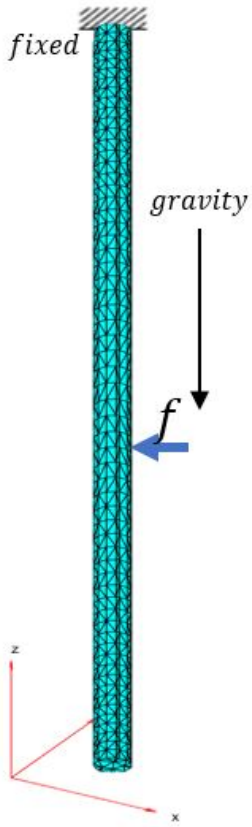

FIGURE 4.1: Illustration of simulation system setup

experiment through the parameter identification step, which will be introduced in Chapter 5.

For the general shaped elastic object, we considered the actuation force is given solely from external environment because there is no internal actuation for this

kind of elastic object. As shown in figure 4.1 silicone bar is held at one fixed end in z direction. Gravitational force is acting in z direction. We divided entire object into 10 pieces along longitudinal direction, and considered these pieces as possible input groups. For this simulation, we assumed that external disturbance is applied at specific position with random magnitude, which will be included in one of possible input groups. BMR is conducted for each input groups. Then, we chose corresponding reduced state for given external disturbance.

Simulation is performed by MATLAB with mesh generated from STL file. For full order model, we adopted 2130 nodes, so the total dimension of full order state is $x \in \mathbb{R}^{6390}$(represents each nodes x, y, z position). $M, K \in \mathbb{R}^{6390\times6390}$ is constructed based on selected material property and given mesh, C is constructed with M, K based on Rayleigh damping.

To check the performance of optimization based estimation algorithm, we first perform full order FEM simulation with PMI integration from (2.3) to use as a ground truth for simulation.

$$\left(\frac{M}{T} + \frac{C}{2} + \frac{KT}{4}\right) x_{k+1} + \left(-\frac{M}{T} + \frac{C}{2} + \frac{KT}{4}\right) x_k + Kx_k = A_e f_{e,k} \tag{4.1}$$

We chose the $T = 0.001s$ for one time step and used the randomly generated disturbance force for $f_{e,k}$. Then, we placed imaginary IMU sensors on the elastic

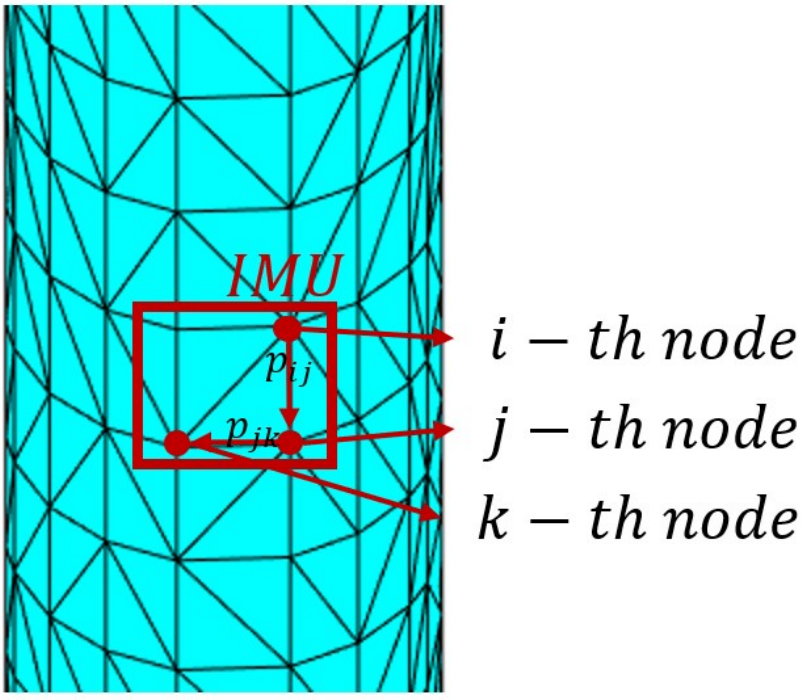

FIGURE 4.2: Illustration of IMU placement

object. The IMU sensors are rigidly attached to soft object, therefore, the nodes placed on the surface which is attached to IMU, can be considered as rigid plates.

We assumed that soft robot's acceleration is small enough. Therefore, we can get rotation matrix of IMU at time t $R_{0,IMU}(t)$ from IMU acceleration data. From FEM model rest position we can find $p_{ij,0}(0)$. Then, using $R_{0,IMU}(0)$ we can find $p_{ij,IMU}(0)$. The under script 0 denotes that reference frame is world frame

and IMU denotes reference frame is IMU frame. For $p_{ij,0}(t)$ we can find following

$$\begin{aligned} p_{ij,0}(t) &= R_{0,IMU}(t)\, p_{ij,IMU}(t) \\ &= R_{0,IMU}(t)\, p_{ij,IMU}(0) \end{aligned} \tag{4.2}$$

Therefore, we can find $p_{ij,0}(t)$ with IMU measurement. Then we can represent measurements with $p_{ij,0}$ and $p_{jk,0}$ as following as (3.2).

$$\begin{aligned} y &= Hx + v \\ H &= \begin{bmatrix} \cdots & -I_{3\times3} & \cdots & I_{3\times3} & \cdots & \cdots & \cdots \\ \cdots & \cdots & \cdots & -I_{3\times3} & \cdots & I_{3\times3} & \cdots \end{bmatrix} \end{aligned} \tag{4.3}$$

Without loss of generality we assume $i < j < k$. Then, for the first three rows, the first $I_{3\times3}$ corresponds to $i-th$ node, $-I_{3\times3}$ corresponds to $j-th$ node. In last three rows, $I_{3\times3}$ represents $j-th$ node, and $-I_{3\times3}$ corresponds to $k-th$ node. When multiple IMU is used, we can construct observation matrix by stacking (4.3).

From this observation matrix, observability gramian can be easily constructed. Sensor placement optimization process is done by maximizing the minimum singular value of observability gramian[25].

From the optimization process, for this simulation, two IMU sensors are chosen, and placed at $0.14(m)$, $0.9(m)$ from the fixed end. The measurement is obtained from the full order simulation (4.1), observation matrix(4.3), and noise (3.2).

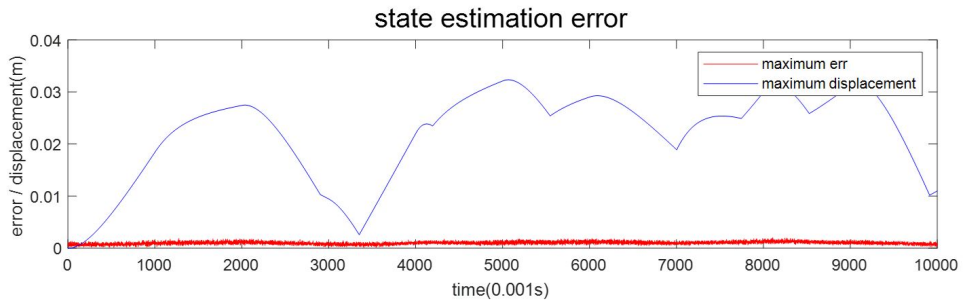

FIGURE 4.3: State estimation error

Then the estimation algorithm (3.4)is performed to find state estimation. After state estimation, we projected the state into the disturbance space and performed force estimation (3.5). The result is shown in figure 4.3,4.4,4.5,4.6.

The state estimation is performed by minimizing the cost function, which is formulated using measurements error and energy cost (3.3),(3.4). This optimization result is not smooth as shown in figure 4.4 because of sensing noise and potential energy term. Therefore, applying this result directly to force estimation would fail. In order to smoothen state estimation result, we projected estimated state to disturbance space (3.5) as shown in 4.5.

Although the state estimation performed well, the force estimation performance in z-direction was poor. This is because the force estimation is performed from the projected state estimation result. The $z-$direction force is in the nullspace of the projection matrix($K^{-1}A_e$) in (3.5). In other words, this force does not affect the state of soft object, so it can be neglected in perception for control sense.

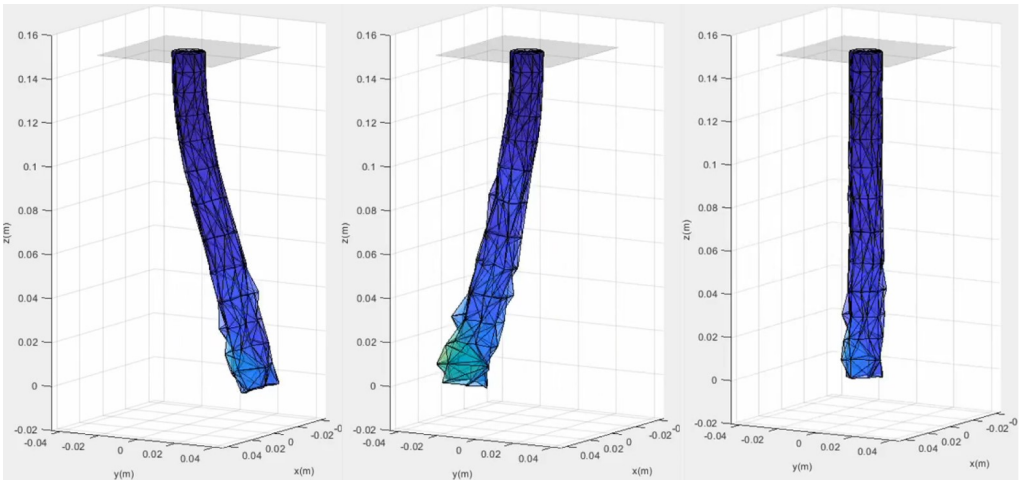

FIGURE 4.4: Noisy state estimation result before projection

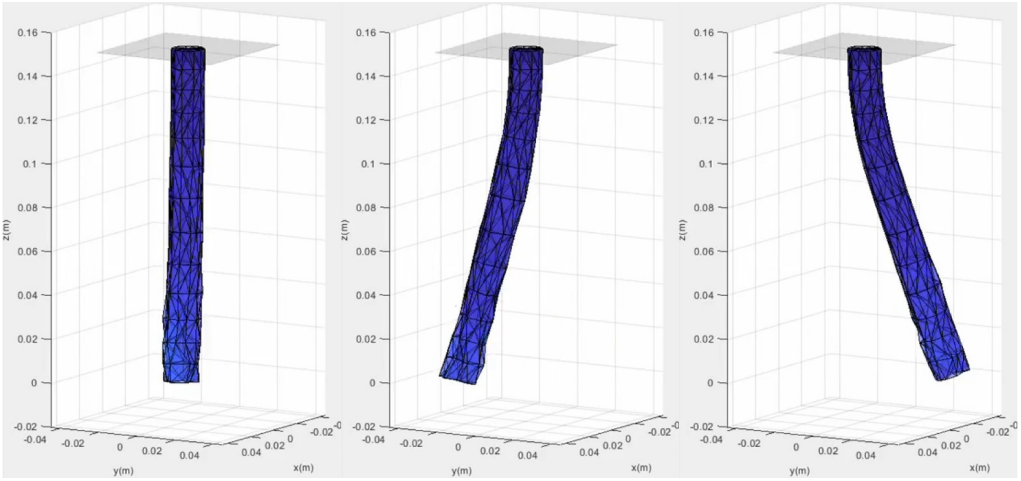

FIGURE 4.5: Smoothed state estimation result after projection

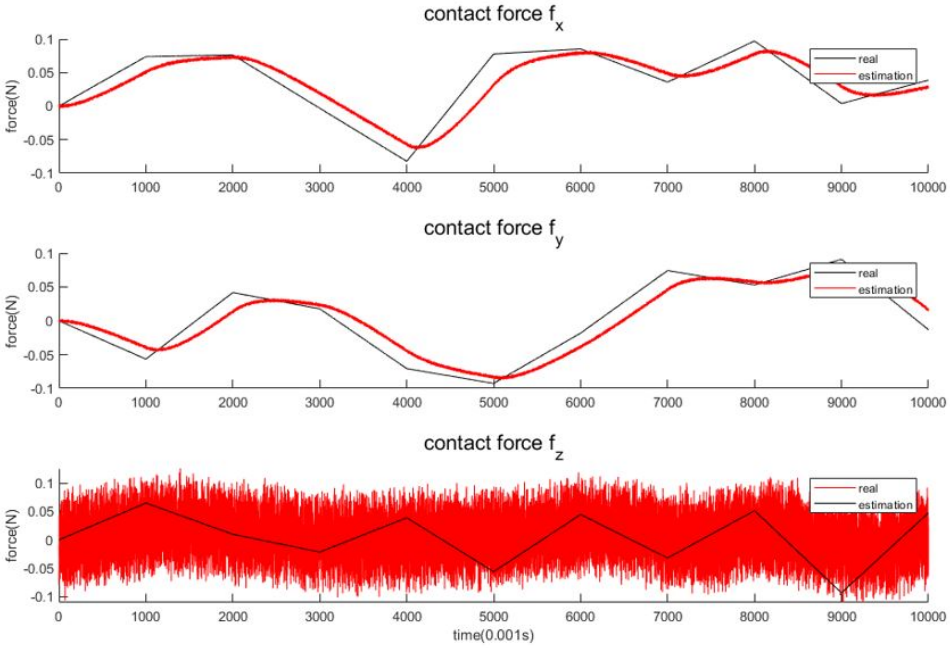

FIGURE 4.6: Force estimation result

4.2 Soft Robot Simulation

For soft robot simulation, we chose simple PneuNet[26],[27] structure to check the performance of filtering based estimation algorithm. We chose this structure because it is well known actuator. However, this algorithm can be applied to other general shaped soft robot because there is no additional assumptions about shape. We considered this PneuNet actuator acts as soft manipulator, and the end effector interacts with environments. Then, with the estimation process, we

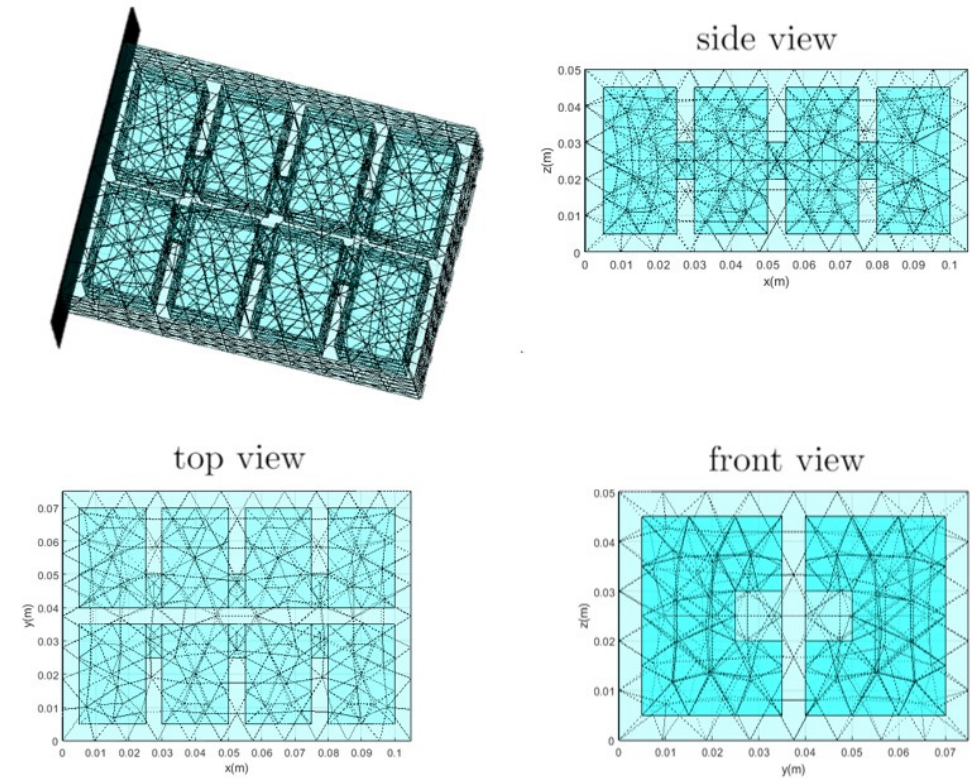

FIGURE 4.7: Illustration of soft robot model used for simulation

can reconstruct the state and interaction force, which can be used to increase the performance of soft robot control by incorporating feedback.

As shown in figure 4.7, the soft robot is fixed in one end, and two actuation chamber actuates the soft robot, which makes the bending motion. We considered the opposite end as end effector. For simplicity, we adopted one segment for

simulation, but it can be easily expanded to soft robots contain multiple segment, by using same filtering based algorithms for each soft robot actuator segments.

For measurements we adopted pressure sensor for actuation, and IMU sensors. Sensor placement optimization is performed same as the process in 3.1. For each IMU placement, the observation matrix can be constructed as (4.3). Then using this observation matrix, we constructed observability gramian, and choose optimal sensor placement that maximizes the minimum singular value of observability gramian.

Then we perform BMR for model reduction. For one PneuNet segment, nodes which lies in internal actuation chamber surfaces and end effector are considered as input nodes, and we constructed input matrix A_e and P_a in (3.6). M, K and C matrix is constructed as the same process done in 3.1. Finally, BMR is performed with constructed soft robot dynamics. For this system, the full order FEM model dimension is $x \in \mathbb{R}^{7218}$ with 2406 nodes, and the reduced mode state dimension with 99.9% Hankel value is 6.

For the performance analysis of filtering based algorithm, we compared the full-order simulation results and estimation results based on the measurements which were collected from full-order simulation. Again, we adopted PMI integration for full order simulation as (4.1).

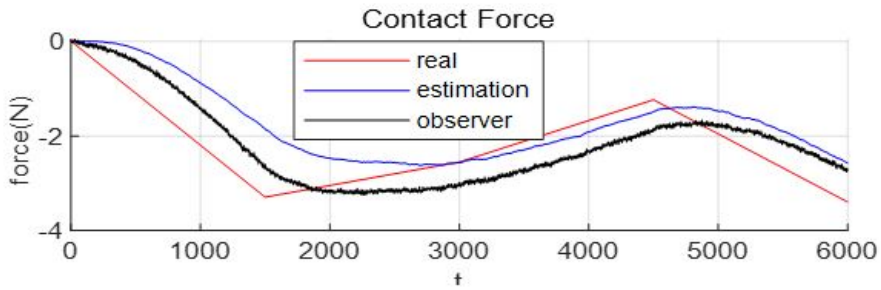

FIGURE 4.8: Force estimation result. Red line indicates full-order simulation result, blue is estimation with filtering, and black indicates force estimation with momentum based observer

$$\left(\frac{M}{T}+\frac{C}{2}+\frac{KT}{4}\right)x_{k+1}+\left(-\frac{M}{T}+\frac{C}{2}+\frac{KT}{4}\right)x_k+Kx_k=A_e f_{e,k}+P_{a,k} \quad (4.4)$$

For simulation, we chose $T = 0.001(s)$ for time step. Actuation $P_{a,k}$ and contact force $f_{e,k}$ is randomly generated. Then, measurements are obtained based on this simulation result, sensor placement optimization, and sensor noise. Estimation results are shown in figure 4.8, 4.9. For additional loop we estimated the external force based on estimated state with momentum based observer[28]. Estimated force with observer and filtering is both Gaussian distribution, so can be fused. This will be dealt with future work.

The estimated force has a time delay compared to full order simulation because we modeled external force as random walk in (3.11).

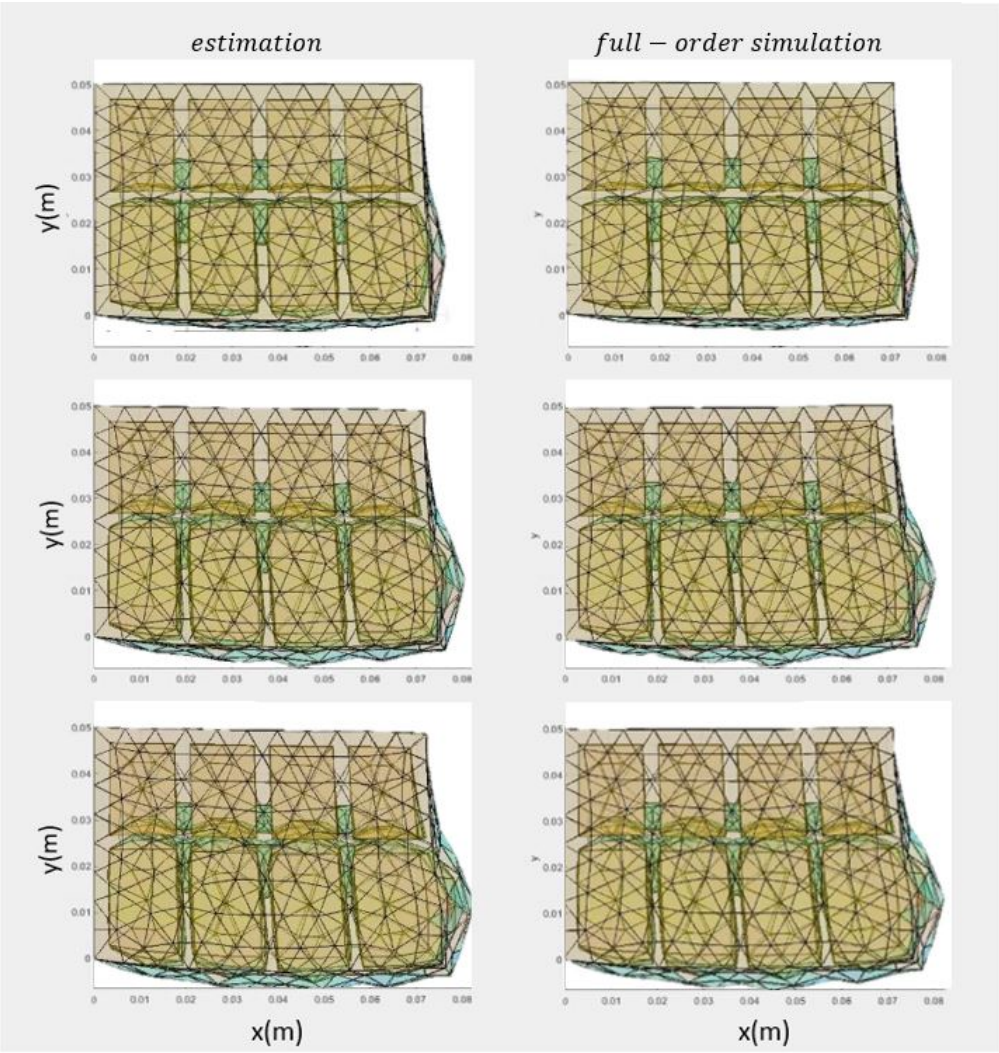

FIGURE 4.9: Snapshot of state estimation result. Left column represents result from full order simulation, and right column shows corresponding estimation result

Chapter 5

Experiments

5.1 Fabrication of Soft Robot

To check our algorithm works on real world system we constructed a soft robot and performed a state and force estimation experiment. Fabrication of soft robot is processed through casting into a mold using a silicone elastomer(EcoFlex 0050) as depicted in figure 5.1. For each segment of soft robot, fabrication step is as following. 1)Mix silicone elastomer and pour it into the mold. 2)Wait 3 hours for curing and demold each pieces. 3)Embed IMU sensors and insert silicone tubes on the silicone body. 4)Use and adhesive(Sil-Poxy, Smooth-On. Inc) to put pieces together.

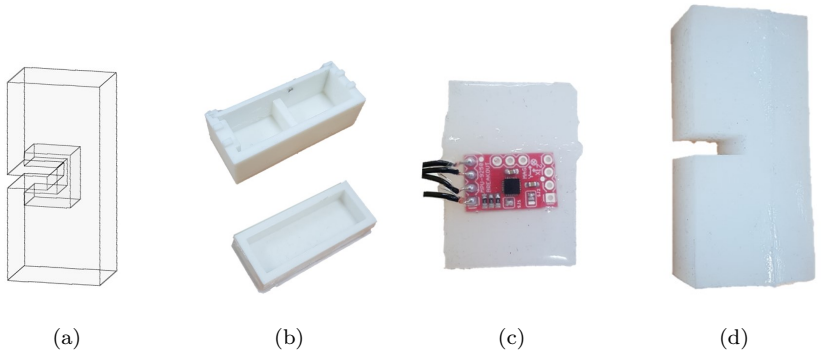

FIGURE 5.1: Illustration of soft robot fabrication (a)Soft robot CAD rendering, (b)Mold, (c)Sensor embedding, (d)Completed segment

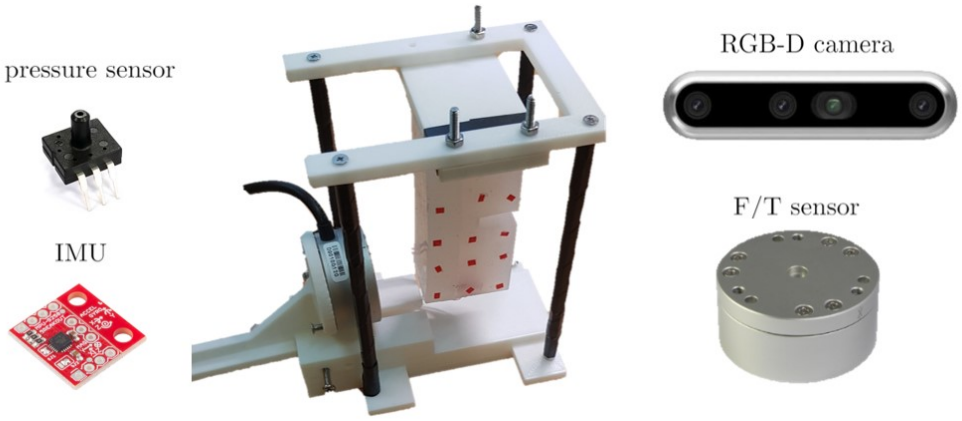

FIGURE 5.2: Experiment setup

For actuation and soft robot sensing, we placed pressure sensor(33A-005G-2210) in the silicone tube and embedded IMU sensors(mpu-9250, sparkfun imu break-out) on soft robot. To verify the accuracy of algorithm, we implemented RGB-D camera(RealSense depth camera D-435, Intel) for shape sensing and force torque

sensor(RFT40-SA01, Robotous) to sense the contact force. 15 markers with random size are placed on the soft robot surface to be tracked by camera.

5.2 Parameter Identification

In order to validate material properties such as Young's modulus, poison's ratio, and Rayleigh damping coefficients we conducted three different steps. 1)Finding the marker positions on the soft robot segment. 2)Quasi-static motion experiment to find Young's modulus, density, and poison's ratio. 3)Dynamic motion experiment to find Rayleigh damping coefficients.

For marker position on soft robot verification, we compared the marker position pointcloud data in rest state with FEM model. For each marker we found tetrahedral element that contains the marker. Then, the marker position can be represented by the interpolation of the nodes in that element as shown in figure 5.3,5.4.

$$p^i_{m,e} = a^i p^i_1 + b^i p^i_2 + c^i p^i_3 \tag{5.1}$$

Where $p^i_{m,e} \in \mathbb{R}^{3\times 1}$ represents ith marker position attained from experiment. Then, from (5.1) we can find the interpolation matrix T_m which maps FEM

FIGURE 5.3: Illustration of tracking marker from RGB-D pointcloud. Picture of soft robot(left), marker tracking in pointcloud data(middle), marker matching to FEM model(right)

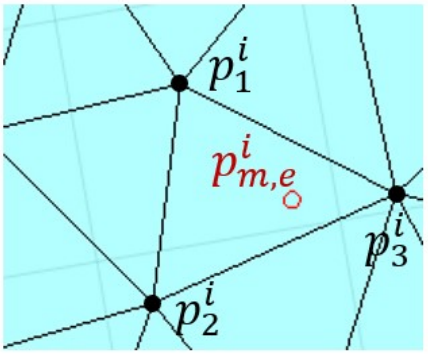

FIGURE 5.4: Illustration of ith marker interpolation

selected node position to marker position and selection matrix S_m by following.

$$T_i = \begin{bmatrix} a^i & 0 & 0 & b^i & 0 & 0 & c^i & 0 & 0 \\ 0 & a^i & 0 & 0 & b^i & 0 & 0 & c^i & 0 \\ 0 & 0 & a^i & 0 & 0 & b^i & 0 & 0 & c^i \end{bmatrix}, \; T_m = diag\left(T_1, T_2, T_3, \cdots\right) \tag{5.2}$$

$$\begin{bmatrix} p_1^1 \\ p_2^1 \\ p_3^1 \\ p_1^2 \\ \vdots \end{bmatrix} = S_m x,\ p_{m,e} = \begin{bmatrix} p_{m,e}^1 \\ p_{m,e}^2 \\ p_{m,e}^3 \\ \dots \end{bmatrix} \tag{5.3}$$

From (5.3), (5.4), we can find marker position from simulation node position $x(k)$, where k means timestep as following

$$p_{m,s}(k) = T_m S_m x(k) \tag{5.4}$$

Then, we conduct a quasi-static experiment. Segment is actuated 0 to 20(kPa) slowly for 5 seconds. With the actuation pressure data, we can find the marker position as a function of Young's modulus, density, and poison's ratio with static equation. Then optimization process is performed to find the optimal value that minimizes the cost function.

$$\begin{aligned} p_{m,s}(\tau) &= f(\nu, E, \rho) \\ \min_{\nu,E,\rho}(cost) &= \|p_{m,e}(\tau) - p_{m,s}(\tau)\| \end{aligned} \tag{5.5}$$

Where ν, E, ρ represents poison's ratio, Young's modulus, and density. $p_{m,e}(\tau)$,$p_{m,s}(\tau)$ $\in \mathbb{R}^{3m \times T_s}$ each denotes the marker position matrix of experiment and simulation where m is number of markers, T_s is total simulation step and τ represents the

experiment scenario (i.e. $p_{m,s}(\tau) = [p_{m,s}(0)\, p_{m,s}(1) \cdots])$. We chose the range of each variables based on material property table of silicone rubber.

With this optimization result,we can construct M and K matrix. Then, we conduct dynamic optimization process. Soft robot is actuated with random actuation with nominal speed. With this data, we denote the marker position as a function of Rayleigh damping coefficientsa, b, and find the optimal coefficients to find the damping matrix $C = aM + bK$.

$$\begin{aligned} p_{m,s}\left(\tau'\right) &= f\left(a, b\right) \\ \min_{a,b}\left(cost\right) &= \|p_{m,e}\left(\tau'\right) - p_{m,s}\left(\tau'\right)\| \end{aligned} \tag{5.6}$$

5.3 Algorithm Validation

After the parameter identification process, BMR is performed with the updated material properties. From the IMU and pressure sensor measurements we applied the filtering based estimation (3.11). Validation of algorithm is performed by checking the accuracy of state estimation and force estimation result. State estimation accuracy is conducted by comparing the position of marker attained from experiment and by interpolation from estimation result as (5.4), and the result is shown in figure 5.6. Force estimation accuracy is checked by comparing the force estimate with force measurement from force torque sensor, and the result is depicted in figure 5.7.

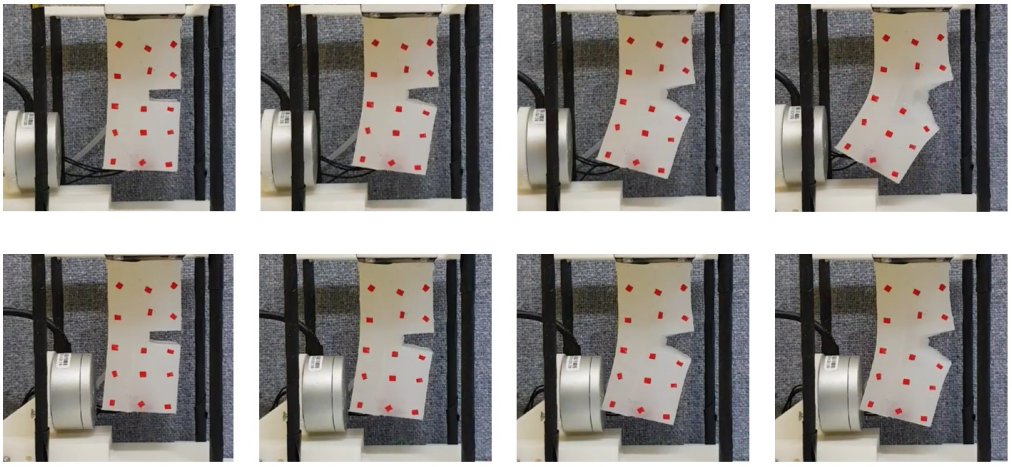

FIGURE 5.5: Snapshot of experiment. Upper 4 pictures show actuation without external force and below 4 pictures show actuation with external force(contact)

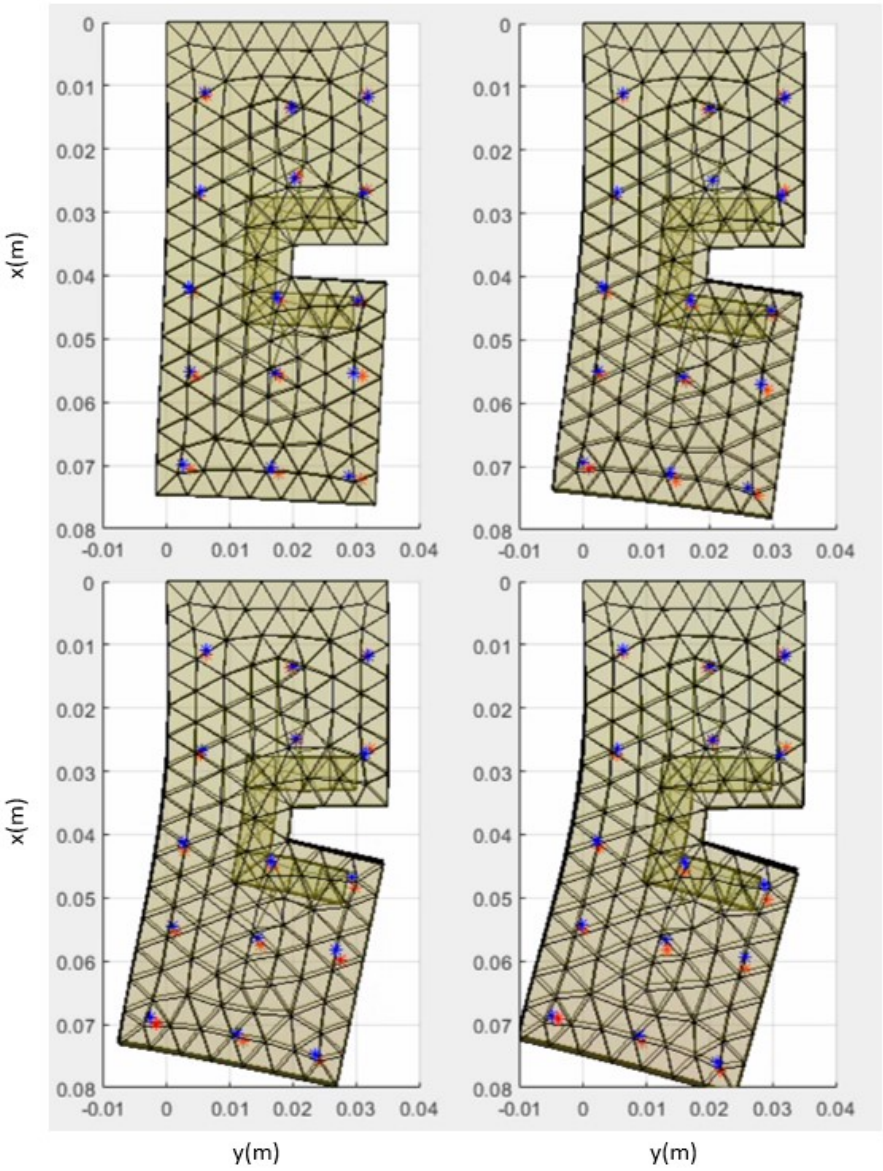

FIGURE 5.6: Snapshot of state estimation result. Red dot indicates marker position from experiment and blue dot indicates from estimation result

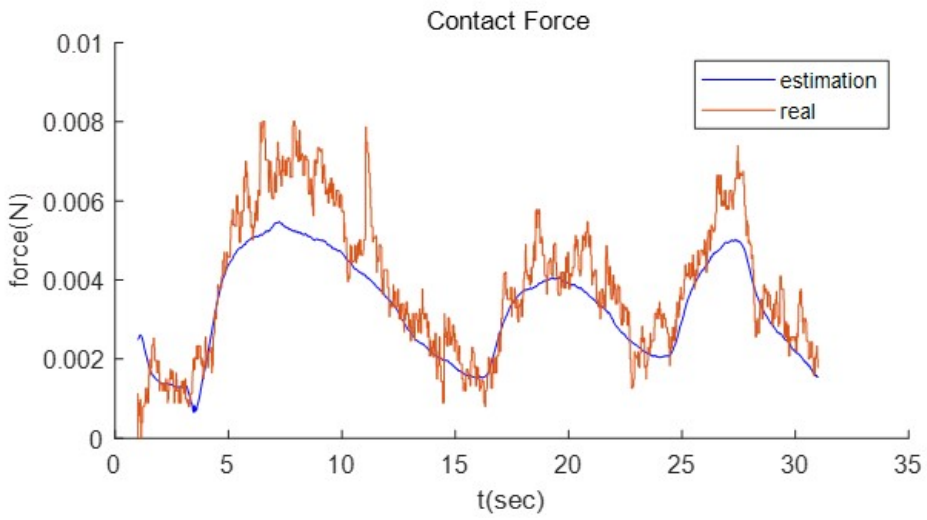

FIGURE 5.7: Force estimation result. Blue indicates estimation result, and red is for experiment result

Chapter 6

Conclusion and Future Work

6.1 Conclusion

In this thesis, we propose algorithms that can enables soft robot's perception. We adopted FEM modelling with BMR and model switching for fast and accurate system modelling. Based on this dynamics, estimation algorithms are developed. For the case of simple soft object without internal actuation we composed cost function consists measurement error with potential energy term. State estimation is done by minimizing this cost function. Then, the state estimation is projected to disturbance space and disturbance estimation is conducted through quasi-static assumption. For the case of soft robot, which has internal actuation, we

adopted filtering based method with augmented state and assuming disturbance as random walk.

Through simulation in Sec. 4 and experiments in Sec. 5, we validated our algorithms and checked it works in real world.

6.2 Future Work

Future work includes the application of model switching algorithm and nonlinear FEM such as co-rotational FEM modelling with corresponding model reduction algorithms. For disturbance estimation we modeled external force as a random walk process. However, as mentioned above incorporating momentum based observer technique, the disturbance force is modeled as first order equation and can be fused with filtering based result to improve the estimation accuracy.

Bibliography

[1] Chiwon Lee, Myungjoon Kim, Yoon Jae Kim, Nhayoung Hong, Seungwan Ryu, H Jin Kim, and Sungwan Kim. Soft robot review. *International Journal of Control, Automation and Systems*, 15(1):3–15, 2017.

[2] Daniela Rus and Michael T Tolley. Design, fabrication and control of soft robots. *Nature*, 521(7553):467–475, 2015.

[3] Michael T Tolley, Robert F Shepherd, Bobak Mosadegh, Kevin C Galloway, Michael Wehner, Michael Karpelson, Robert J Wood, and George M Whitesides. A resilient, untethered soft robot. *Soft robotics*, 1(3):213–223, 2014.

[4] Hongbo Wang, Massimo Totaro, and Lucia Beccai. Toward perceptive soft robots: Progress and challenges. *Advanced Science*, 5(9):1800541, 2018.

[5] Thomas George Thuruthel, Benjamin Shih, Cecilia Laschi, and Michael Thomas Tolley. Soft robot perception using embedded soft sensors and recurrent neural networks. *Science Robotics*, 4(26), 2019.

[6] Javier Tapia, Espen Knoop, Mojmir Mutnỳ, Miguel A Otaduy, and Moritz Bächer. Makesense: Automated sensor design for proprioceptive soft robots. *Soft robotics*, 7(3):332–345, 2020.

[7] Ruoyu Wang, Shiheng Wang, Songyu Du, Erdong Xiao, Wenzhen Yuan, and Chen Feng. Real-time soft body 3d proprioception via deep vision-based sensing. *IEEE Robotics and Automation Letters*, 5(2):3382–3389, 2020.

[8] Robert K Katzschmann, Cosimo Della Santina, Yasunori Toshimitsu, Antonio Bicchi, and Daniela Rus. Dynamic motion control of multi-segment soft robots using piecewise constant curvature matched with an augmented rigid body model. In *2019 2nd IEEE International Conference on Soft Robotics (RoboSoft)*, pages 454–461. IEEE, 2019.

[9] Cosimo Della Santina, Ryan Landon Truby, and Daniela Rus. Data–driven disturbance observers for estimating external forces on soft robots. *IEEE Robotics and Automation Letters*, 5(4):5717–5724, 2020.

[10] Ryan L Truby, Cosimo Della Santina, and Daniela Rus. Distributed proprioception of 3d configuration in soft, sensorized robots via deep learning. *IEEE Robotics and Automation Letters*, 5(2):3299–3306, 2020.

[11] John Till, Vincent Aloi, and Caleb Rucker. Real-time dynamics of soft and continuum robots based on cosserat rod models. *The International Journal of Robotics Research*, 38(6):723–746, 2019.

[12] Zhongkai Zhang, Jérémie Dequidt, and Christian Duriez. Vision-based sensing of external forces acting on soft robots using finite element method. *IEEE Robotics and Automation Letters*, 3(3):1529–1536, 2018.

[13] Yu She, Sandra Q Liu, Peiyu Yu, and Edward Adelson. Exoskeleton-covered soft finger with vision-based proprioception and tactile sensing. In *2020 IEEE International Conference on Robotics and Automation (ICRA)*, pages 10075–10081. IEEE, 2020.

[14] Yazhan Zhang, Zicheng Kan, Yang Yang, Yu Alexander Tse, and Michael Yu Wang. Effective estimation of contact force and torque for vision-based tactile sensors with helmholtz–hodge decomposition. *IEEE Robotics and Automation Letters*, 4(4):4094–4101, 2019.

[15] Klaus-Jürgen Bathe. *Finite element procedures*. Klaus-Jurgen Bathe, 2006.

[16] J. Yoon, I. Hong, and D. Lee. Passive model reduction and switching for fast soft object simulation with intermittent contacts. In *2019 IEEE/RSJ International Conference on Intelligent Robots and Systems (IROS)*, pages 6963–6970, 2019. doi: 10.1109/IROS40897.2019.8968132.

[17] Hervé Abdi and Lynne J Williams. Principal component analysis. *Wiley interdisciplinary reviews: computational statistics*, 2(4):433–459, 2010.

[18] Clarence W Rowley. Model reduction for fluids, using balanced proper orthogonal decomposition. *International Journal of Bifurcation and Chaos*, 15(03):997–1013, 2005.

[19] Olivier Goury and Christian Duriez. Fast, generic, and reliable control and simulation of soft robots using model order reduction. *IEEE Transactions on Robotics*, 34(6):1565–1576, 2018.

[20] Kanti Bhushan Datta. Linear system theory and design, by chi-tsong chen, oxford university press, new york, 1999, 334 pages, isbn 0-19-511777-8, 2000.

[21] Karen Willcox and Jaime Peraire. Balanced model reduction via the proper orthogonal decomposition. *AIAA journal*, 40(11):2323–2330, 2002.

[22] J. Ahn, J. Yoon, J. Lee, and D. Lee. Model-free optimal estimation and sensor placement framework for elastic kinematic chain. In *2019 International Conference on Robotics and Automation (ICRA)*, pages 8776–8782, 2019. doi: 10.1109/ICRA.2019.8793665.

[23] Myungsin Kim, Yongjun Lee, Yongseok Lee, and Dongjun Lee. Haptic rendering and interactive simulation using passive midpoint integration. *The International Journal of Robotics Research*, 36(12):1341–1362, 2017.

[24] Dongjun Lee and Ke Huang. On passive non-iterative variable-step numerical integration of mechanical systems for haptic rendering. In *Dynamic Systems and Control Conference*, volume 43352, pages 1147–1154, 2008.

[25] Didier Georges. The use of observability and controllability gramians or functions for optimal sensor and actuator location in finite-dimensional systems. In *Proceedings of 1995 34th IEEE Conference on Decision and Control*, volume 4, pages 3319–3324. IEEE, 1995.

[26] Bobak Mosadegh, Panagiotis Polygerinos, Christoph Keplinger, Sophia Wennstedt, Robert F Shepherd, Unmukt Gupta, Jongmin Shim, Katia Bertoldi, Conor J Walsh, and George M Whitesides. Pneumatic networks for soft robotics that actuate rapidly. *Advanced functional materials*, 24(15): 2163–2170, 2014.

[27] Tao Peng, Bork A Berghoff, Jeong-Il Oh, Lennart Weber, Jasmin Schirmer, Johannes Schwarz, Jens Glaeser, and Gabriele Klug. Regulation of a polyamine transporter by the conserved 3′ utr-derived srna sorx confers resistance to singlet oxygen and organic hydroperoxides in rhodobacter sphaeroides. *RNA biology*, 13(10):988–999, 2016.

[28] Wen-Hua Chen, Jun Yang, Lei Guo, and Shihua Li. Disturbance-observer-based control and related methods—an overview. *IEEE Transactions on industrial electronics*, 63(2):1083–1095, 2015.

요약

본 논문에서는 온보드 센서 기반 소프트 로봇의 실시간 상태 및 외력추정 알고리즘의 개발에 대해서 기술한다.

유한요소방법을 기반으로 소프트로봇을 모델링하였고 이를 모델 축소와 모델 스위칭 기법을 사용하여 실시간 연산을 가능하게 하였다. 자체 액츄에이션이 없는 경우 에너지와 측정 에러를 코스트로 하여 최적화 기법을 통해 형상추정을 진행하였고 이를 변위공간에 투영하여 외력추정을 하는 알고리즘을 개발하였다. 자체 액츄에이션이 있는 경우 외력을 랜덤워크로 모델링하여 필터링 기반으로 상태와 외력을 동시추정하는 알고리즘을 개발하였다. 개발한 알고리즘은 시뮬레이션과 제작된 소프트로봇을 통하여 검증되었다.

주요어: Balanced model reduction, Finite element method, Optimization, Filtering, Soft robotics
학번:2018-21160